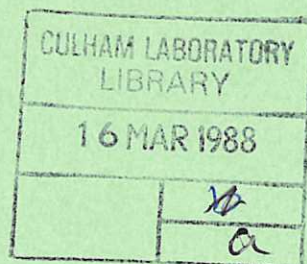


CULHAM LIBRARY
REFERENCE ONLY



Improved confinement in HBTX with removal of tile limiters

B. Alper
C.A. Bunting
J. Cunnane
A. R. Field
A. Lazaros
P. G. Noonan
H. Y. W. Tsui

H. A. B. Bodin
P. G. Carolan
D. E. Evans
R. J. Hayden
A. A. Newton
A. Patel
P. D. Wilcock



UK ATOMIC ENERGY
AUTHORITY

Culham
Laboratory

This document is intended for publication in a journal or at a conference and is made available on the understanding that extracts or references will not be published prior to publication of the original, without the consent of the authors.

Enquiries about copyright and reproduction should be addressed to the Librarian, UKAEA, Culham Laboratory, Abingdon, Oxon. OX14 3DB, England.

Improved confinement in HBTX with removal of tile limiters

B. Alper	H. A. B. Bodin	C. A. Bunting
P. G. Carolan	J. Cunnane*	D. E. Evans
A. R. Field†	R. J. Hayden*	A. Lazaros‡
A. A. Newton	P. G. Noonan	A. Patel
H. Y. W. Tsui	P. D. Wilcock	

Culham Laboratory, Abingdon, Oxon, OX14 3DB, UK
(UKAEA/Euratom Fusion Association)

*University College, Cork, Ireland

†Royal Holloway and Bedford New College, London

‡UMIST, Manchester

ABSTRACT

Removing the limiters from the HBTX experiment has had the beneficial effect of reducing the loop voltage by about a third. Since the poloidal beta, β_θ , remains largely unaltered there is a corresponding 50% improvement in the energy confinement time. Soft X-ray measurements show a suprathreshold tail in the electron energy distribution for the first time. The 156 graphite tiles cover about 8% of the vacuum vessel and protrude 1 cm into the plasma. The consequent drop in loop voltage with their removal is in agreement with models for the loop voltage based on global magnetic helicity balance. The observed changes in the ion temperature are consistent with these models when the energy balance of electrons and ions is also included.

(To be published in Plasma Physics and Controlled Fusion)

Culham Laboratory
United Kingdom Atomic Energy Authority
Abingdon
Oxfordshire OX14 3DB

October 1987

INTRODUCTION

The characteristics of the edge region in Reversed Field Pinch (RFP) plasmas are found to have a strong influence on the global properties of the plasma. For example, reducing the field errors in the HBTX series of experiments (ALPER et al, 1986), decreases the loop voltage and increases both the energy confinement time and the plasma duration. These improvements followed reductions in the toroidal field ripple and the field errors at the ports and shell gaps. The poloidal flux intersecting the liner, for uncentred RFP plasmas, can also be considered as a field error and its reduction, using a DC vertical field, gives further improvements (NOONAN et al, 1985). These improvements are much greater than those expected from changes in plasma aperture, electron temperature (T_e) or impurity concentration. Furthermore, localised perturbations of the plasma boundary due to the presence of material objects (eg graphite limiter tiles) can result in increases in the plasma resistance, Ω , which cannot be explained in terms of Spitzer resistivity (including Z_{eff} from impurities) (ALPER and TSUI, 1987a; CAROLAN et al, 1987a)

In RFP's it is often not straight-forward to account for global plasma resistance Ω in terms of resistivity and current density profiles. For example, when the resistivity on axis, η_0 , is derived from Ω using helicity balance it differs substantially from the Spitzer value by a factor ≥ 3 , ie. well outside experimental errors. This is particularly important under conditions of large field errors (high loop voltage) or at high electron temperatures where unrealistic values of Z_{eff} would be required to account for Ω in the conventional way. This is in contrast to plasmas with low values of T_e where the Spitzer η_0 is large and may therefore dominate effects from field errors which can be masked by the experimental uncertainties.

Models to account for the resistivity based on magnetic helicity balance, as applied to relaxed state systems, have been developed (JARBOE and ALPER, 1987; TSUI, 1987) to account for the observed dependence of Ω , or loop voltage, V_ϕ , on field error and plasma boundary perturbations. These models yield results in approximate agreement with experiment and so give further support to the idea that the plasma edge is important in determining V_ϕ in an RFP.

HELICITY BALANCE

In a quasi-force-free configuration the current density, \underline{j} , and the magnetic fields, \underline{B} , are almost parallel. In determining the

Spitzer loop-voltage, it is necessary to include the dynamo electric field which drives the poloidal current and gives B_θ and B_ϕ profiles that are consistent with observations. The favoured approach links the on-axis resistivity, η_0 , and Ω through helicity balance (SCHOENBERG et al, 1984; TSUI et al, 1986). The magnetic helicity, K , of the plasma is defined by (BEVIR and GRAY, 1981)

$$K = \int \underline{A} \cdot \underline{B} \, d^3x - \oint \underline{A} \cdot d\alpha \oint \underline{A} \cdot d\beta \quad (1)$$

where \underline{A} is the vector potential related to the magnetic field \underline{B} through $\underline{B} = \nabla \times \underline{A}$ and $\underline{\alpha}$ and $\underline{\beta}$ are poloidal and toroidal unit vectors.

The rate of change of magnetic helicity, \dot{K} , of the plasma is

$$\dot{K} = 2V_\phi \Phi - 2 \int \underline{E} \cdot \underline{B} \, d^3x \quad (2)$$

where Φ is the toroidal flux and \underline{E} the electric field, which, in the steady-state when $\dot{K}=0$, gives

$$V_\phi \Phi = \int \underline{E} \cdot \underline{B} \, d^3x \quad (3)$$

On the basis of a recent model put forward to explain the observed values of V_ϕ on HBTX (JARBOE and ALPER, 1987) it is suggested that most of the helicity dissipation (~75%, typically) occurs in the small plasma edge volume containing field lines which intersect the vessel wall with only a smaller fraction (~25%) dissipated in the bulk plasma. Dividing the plasma volume into a core and edge region we may write (3) in the form

$$V_\phi \Phi = \int_{\text{core}} \underline{E} \cdot \underline{B} \, d^3x + \int_{\text{edge}} \underline{E} \cdot \underline{B} \, d^3x \quad (4)$$

which yields an additional voltage, ΔV_ϕ , above the Spitzer value of

$$\begin{aligned} \Delta V_\phi &\approx E_\parallel \frac{B_\theta(a)}{\Phi} \cdot 2\pi R \cdot 2\pi a \, \Delta r, \text{ for } |B_\theta(a)| \gg |B_\phi(a)| \\ &= E_\parallel \left(\frac{\Theta}{\pi a^2} \right) 4\pi^2 R a \, \Delta r \end{aligned} \quad (5)$$

where Δr is the penetration depth of the field error, R and a are the major and minor radii of the liner, $4\pi^2 R a \Delta r$ the associated edge volume appropriate to toroidally symmetric cases and Θ is the usual pinch parameter $= B_\theta(a) \pi a^2 / \Phi$. The electric field E_\parallel , parallel to the edge

magnetic field is not necessarily constant along a field line and may be considered here as a time and volume average consistent with the second integral of (4). Without attempting to account for the physical origin of E_{\parallel} , the model is applied to results from HBTX1A/1B (where V_{ϕ} ranged from 30 V to 100 V) to determine its magnitude. A single value of E_{\parallel} ($= 27 \pm 7$ V/m) can account for the results in a range of different conditions (JARBOE and ALPER, 1987).

A physically different approach but also based on helicity balance (TSUI, 1987) is to include the helicity loss through the plasma boundary when $\underline{B} \cdot \underline{n} \neq 0$, where \underline{n} is a unit area vector. The analysis starts from equation (1) and explicitly includes a term to represent the (unknown) gauge associated with A, ie. $\dot{\underline{A}} = -(\underline{E} + \nabla\chi)$, where χ has dimensions of electric potential. In a steady state equation (3) then becomes

$$V_{\phi} \Phi = \int_V \underline{E} \cdot \underline{B} d^3x + \int_S \chi \underline{B} \cdot \underline{n} d^2x \quad (6)$$

where s is the boundary surface of the plasma and v the corresponding volume. When \underline{B} crosses the surface (eg. due to a field error) and if there is a potential difference $\Delta\chi$ between the point of entry and exit of the field line at the surface, then the increase in ΔV_{ϕ} , when $B \approx B_{\theta}(a)$, is given by

$$\Delta V_{\phi} = \Delta\chi \frac{\theta}{\pi a^2} \cdot \Delta A \quad (7)$$

where ΔA is the projected area of the surface normal to the field lines. This approach can similarly explain the observed values of V_{ϕ} on HBTX1A/1B with $\Delta\chi = 18 \pm 4$ volts. Furthermore, the value of $\Delta\chi$ can be derived from plasma sheath theory (TSUI, 1987). This gives $\Delta\chi \sim 1.8 T_e$ where $\Delta\chi$ is in volts and T_e is the local electron temperature (in eV). With $\Delta\chi \approx 18$ volts an edge plasma temperature of $T_e \sim 10 \pm 2$ eV can explain the variation of loop voltage with equilibrium shift.

These two approaches describe quite different physics in that the first deals with a phenomenon occurring within the edge plasma, and the second is a purely surface effect. Shafranov equilibrium shift experiments are consistent with either interpretation, which can be seen by equating (5) and (7) and identifying E_{\parallel} numerically with $\Delta\chi/\pi a = 1.8 T_e/\pi a$. In the case of plasmas with no centering vertical field the Shafranov equilibrium shift ($\Delta = a^2/R$, where R is the major radius) gives rise to a corresponding ΔV_{ϕ} . Whether this additional voltage will be easily seen depends on its magnitude relative to the Spitzer voltage. It can be readily shown from (7) that

$$\frac{\Delta V_{\phi}}{I_{\phi} \Omega_C} \propto \frac{T_{e,edge} T_e^{3/2}}{I_{\phi} Z_{eff}} \left(\frac{a^2}{R}\right) \quad (8)$$

where T_e and $T_{e,edge}$ are the electron temperatures of the bulk and edge plasmas respectively and Ω_C is the classical (or Spitzer) plasma resistance. Thus, the additional voltage will be most prominent in discharges with high temperature, large minor radius, small aspect ratio and low impurity content. As HBTX1B has the largest a^2/R of existing RFP machines, and usually operates at high T_e , additional voltages should be more easily observed than in other machines.

RESULTS WITH LIMITER TILES

We now present examples of results from HBTX1B which can be interpreted in terms of these models. For example, in Figure 1, V_{ϕ} is plotted against I_{ϕ} for a narrow range of central $T_e \approx 250 \pm 35$ eV. All data have nominally centred plasmas. Provided changes with current of the profiles $j(r)$, $T_e(r)$ and $Z_{eff}(r)$ are small, then Ω_C should be constant and either (4) or (6) has the form of a straight line:

$$V_{\phi} = \Delta V_{\phi} + I_{\phi} \Omega_C \quad (9)$$

with a non-zero ordinate intercept corresponding to ΔV_{ϕ} which is associated with helicity dissipation at the edge and a slope corresponding to Ω_C . Indeed, as shown in the figure, the data do display such a dependence. A least-squares fit yields a value of $\Delta V_{\phi} \sim 20 \pm 1$ V from the intercept and a value of $\Omega_C \sim 67 \pm 10$ μohm from the slope. This resistance is in good agreement with that calculated from helicity balance (eqn(3)) using a profile of the Spitzer resistivity, assuming $T_e = T_{e0} [1 - (r/a)^4]$, $Z_{eff} = 2$ obtained from spectroscopic and bolometric measurements, and a current profile derived from a Modified Bessel Function Model. The value of Z_{eff} is a bulk average based on a profile which peaks on axis and falls slowly with radius (CAROLAN et al, 1987a).

The helicity balance models thus give a simple explanation of both the values of V_{ϕ} and their dependence on current as displayed in Fig. 1. With the tiles in place, at a fixed current of $I_{\phi} = 220$ kA, the plasma resistance Ω was apparently independent of electron temperature on axis (JARBOE and ALPER, 1987) over the range $200 < T_e < 470$ eV. This is readily explained because the contribution from $\Delta V_{\phi}/I_{\phi}$ dominates any contribution from changes in Ω_C and provides a natural explanation of the high values of resistance anomaly factors found at low densities (ie. high T_e and low Ω_C).

It is difficult, though not impossible to envisage a mechanism applicable to all RFP plasmas that can re-arrange the T_e , Z_{eff} or current profiles, so as to maintain an approximately constant plasma resistance as T_e varies, or produce the linear rise of V_ϕ with I_ϕ as seen in Fig. 1.

MOVEABLE TILE STUDIES

The effect of helicity dissipation from the interception of flux lines by material objects at the boundary was tested in a more controlled manner by inserting a 5cm wide moveable carbon tile into the plasma edge up to 6cm beyond the liner. Two orientations were measured (a) with the field normal to the tile face and (b) edge on to the field. As expected from (5) and (7), V_ϕ is found to increase with insertion depth beyond the fixed limiters (Fig. 2). Also, when the tile is face-on to B_θ , ΔV_ϕ is about three times greater than the edge-on orientation in the ratio of the corresponding areas as expected from (7) only.

As the moveable tile was inserted the ratio T_i/T_e rose with insertion depth from ~ 1 (for no insertion) to ~ 2 at a depth of 6 cm (CAROLAN et al, 1987b; CAROLAN et al, 1987c). This increase in T_i/T_e and the accompanying increase in loop voltage with tile insertion strongly suggests that additional input power is being dissipated in the plasma bulk and is responsible for increased ion heating.

A second smaller tile was inserted into the plasma such that a fixed area of 10cm^2 of flux was always intercepted (ALPER and TSUI, 1987b). In this case V_ϕ was found to rise with insertion depth up to 5cm into the plasma from the edge, followed by a flattening of V_ϕ with deeper insertion. From equation (7) and (TSUI, 1987), for constant flux interception, $\Delta V_\phi \propto T_e$ (measured at the radial position of the tile), so the rise in V_ϕ with insertion depth should reflect a rise in T_e in this region. The T_e profile obtained is broader than the $(1-(r/a)^4)$ form assumed. The absolute value of the rise in V_ϕ per unit area of flux intercepted beyond 5cms was $0.9\text{V}/\text{cm}^2$. From equation (7) this implies a value of $\Delta\chi$ of 1200 ± 200 V corresponding to $T_e \sim 675 \pm 110$ eV for depths $>5\text{cm}$ from the wall. This compares with values of T_e (on-axis) of 475 ± 75 eV measured during similar discharges. Thus better agreement with experiment would be achieved by using $\Delta\chi \sim 2.6 T_e$, rather than derived $\Delta\chi \sim 1.8 T_e$ based on simplified sheath theory.

Changes in impurity fractions in the bulk plasma were negligible except at large insertion depths and at times in the discharge later than when these measurements were made (ALPER and TSUI, 1987a; CAROLAN et al, 1987a). In these cases the further rise in V_ϕ could be

explained classically.

The pinch parameters θ and $F (=B_{\phi}(a)\pi a^2/\Phi)$ remained almost constant ($\theta \sim 1.4$; $F \sim 0.1$) with the tile insertion so that the current density profile, remote from the tile, also remained largely unaltered. Thus the inserted tile is not acting as a limiter in determining the plasma aperture as may also be inferred from the loop voltage dependence on tile orientation.

RESULTS WITH THE LIMITER TILES REMOVED

A reasonable conclusion from the experimental results discussed above and supported by the models is that the 156 fixed tile limiters in HBTX1B were contributing to the excess loop voltage ΔV_{ϕ} and that it would fall with their removal. These tiles were removed from their clip-mounts by means of a mechanical arm inserted through the diagnostic ports. The clips are nominally recessed in the bellows convolutions and in general do not protrude into the plasma. After tile removal and ~ 500 discharges to clean up the plasma and 'condition' the liner, V_{ϕ} fell from the minimum value observed previously with tiles in position of 30 V, down to 18 V at 220 kA.

The experimental dependence of V_{ϕ} and I_{ϕ} is shown in Figure 3 for a narrow range of T_e on axis of 340 ± 35 eV and no limiters. The data can be interpreted similarly to those in Figure 1, in terms of a linear slope and finite ordinate intercept. In this case a least-squares fit to the data yields a value of 10 ± 1 volts for ΔV_{ϕ} and a value for Ω_c of 65 ± 10 μohm . This resistance is also in good agreement with the value calculated for the bulk plasma at this value of T_e with estimated profiles and the increased value for $Z_{eff} \sim 3$ as measured, see below. Similar dependences are found using data at other fixed values of T_e , and are consistent with the same intercept, 10 ± 3 V, a slope which varies classically as $T_e^{-3/2}$ and Z_{eff} values of 2.5 - 4. The reduction in ΔV_{ϕ} by 10 ± 3 V is consistent with predictions of the helicity models, viz 8 ± 2 volts from the calculations of helicity loss across the plasma boundary to the graphite tiles (eqn(7)) and 15 ± 4 volts from helicity dissipation in the edge volume (eqn (5) with $E_{\parallel} = 27\text{V/m}$). The remaining additional voltage after tile removal ($\Delta V_{\phi} \sim 10\text{V}$) could arise from residual field errors but as field geometry and plasma position are not measured to sufficient accuracy, a quantitative account cannot be provided. Radial field fluctuations at the walls may contribute $\sim 5\text{V}$ to the surface term and distortions in the liner geometry, protrusion of some clip mounts and the bellows convolutions (~ 7 mm depth) may also contribute. Fine tuning of the plasma position

(both horizontally and vertically) to less than 5 mm had little effect on the measured residual loop voltage.

Other changes in plasma parameters are listed in Table 1 where average values are compared for groups of discharges with and without tiles at the same current, θ and electron densities. The electron temperature increases and the ion temperature decreases when the tiles are removed. The fall in the T_i/T_e ratio is expected (CAROLAN et al, 1987b) as ion heating, postulated to be associated the $\tilde{u}\tilde{x}\tilde{B}$ fluctuations required to support the bulk and edge helicity loss, has been reduced compared with the ohmic heating of the electrons. However, the poloidal beta, β_θ , has changed little as seen with previous reductions in field errors, and so the energy confinement time depends inversely on V_ϕ ($\tau_E \propto \beta_\theta I_\phi / V_\phi$). Thus, improvements in the boundary region increase the global energy confinement time. The radiated power has increased from about 5% to 12% of the input power and ζ , the X-ray enhancement factor over pure hydrogen bremsstrahlung, shows a similar relative increase from 2 to 4.5. It is important to note that although V_ϕ is reduced, the value of Z_{eff} increases from about 2 to 3 with limiter removal.

In tile-free operation a suprathreshold component in the soft X-ray spectrum corresponding to runaway electrons was seen for the first time in HBTX. It was observed above 3keV in X-ray energy, as shown in Fig 4, under conditions of low current, at high I/N , and low loop voltage i.e. $I_\phi \sim 80$ kA, $I/N \approx 20 \times 10^{-14}$ A m, $V_\phi \sim 9$ V, when the bulk electron temperature on axis was about 600 eV. The tail had a characteristic temperature about 10x thermal.

CONCLUSIONS

The importance of the edge region in determining the loop voltage and energy confinement time in the RFP has been demonstrated by a series of experiments on HBTX. These observations have been interpreted in terms of helicity balance, which is found to provide a useful framework for understanding and a method for predicting the dependence of the measured loop volts and ion heating on field errors, on equilibrium shift, and on the presence of obstructions near the walls.

In particular, the prediction that the removal of the 156 limiter tiles would lead to a reduction by about a factor of 2 in the additional component of loop volts was vividly confirmed when ΔV_ϕ decreased by 10 ± 3 V. This was accompanied by a decrease in T_i and an increase in T_e , no change in β_θ , and an increase in energy confinement time.

ACKNOWLEDGEMENTS

We would like to thank in particular R Hall and M Bains for the in situ removal of the limiter tiles, L Firth for the construction of the moveable tiles and P Bussell and M Butler for the operation and maintenance of the HBTX electrical system.

REFERENCES

- ALPER B, et al (1986) Proceedings of the 11th International Conference on Plasma Physics and Controlled Nuclear Fusion (IAEA, Vienna) Vol. 2, 339
- ALPER B, and TSUI H Y W (1987a) Proceedings of the 14th European Conference on Controlled Fusion and Plasma Physics, Madrid, Part II, 434
- ALPER B, and TSUI H Y W (1987b), Proceedings of the International School of Plasma Physics, Varenna, to be published
- BEVIR M K and GRAY J (1981) Proceedings of Reversed Field Pinch Theory Workshop, Los Alamos, Rep No. LA-8944-Cm, 176
- CAROLAN P G, BUNTING C A, MANLEY A M and PATEL A (1987a) Proceedings of the 14th European Conference on Controlled Fusion and Plasma Physics, Madrid, Part II, 515
- CAROLAN P G, FIELD A R, LAZAROS A, RUSBRIDGE M G, TSUI H Y W and BEVIR M K (1987b) Proceedings of the 14th European Conference on Controlled Fusion and Plasma Physics, Madrid, Part II, 469
- CAROLAN P G, FIELD A R, LAZAROS A, RUSBRIDGE M G, TSUI H Y W and BEVIR M K (1987c) Proceedings of the International School of Plasma Physics, Varenna, to be published
- JARBOE T R and ALPER B, (1987) Physics Fluids 30 1177
- NOONAN P G, TSUI H Y W and NEWTON A A, (1985) Plasma Physics Controlled Fusion 27 1307
- SCHOENBERG M K, MOSES R W and HAGENSON R L (1984) Physics Fluids 27 1671
- TSUI H Y W, NEWTON A A and RUSBRIDGE M G (1986) Proceedings of the 13th European Conference on Controlled Fusion and Plasma Heating, Schliersee, Part I, 345
- TSUI H Y W (1987) Proceedings of the 14th European Conference on Controlled Fusion and Plasma Physics, Madrid, Part II, 473

Table 1

	With Tiles	Without Tiles
I (kA)	220	220
n_e ($\times 10^{19} \text{ m}^{-3}$)	1.5	1.5
F	-0.1	-0.1
θ	1.4	1.4
T_e (eV)	350	460
T_i (eV)	360	230
Ω (μohm)	150	100
V_ϕ (volts)	33	22
β_θ (%)	9	9
τ_E (ms)	0.22	0.33
$P_{\text{rad}}/I \cdot V_\phi$ (%)	5	12
ζ	2	4.5
Z_{eff}	2	3

Table 1 Comparison of plasma parameters averaged over several discharges before and after removal of the tile limiters for a sample of data at similar values of current, density, F and θ .

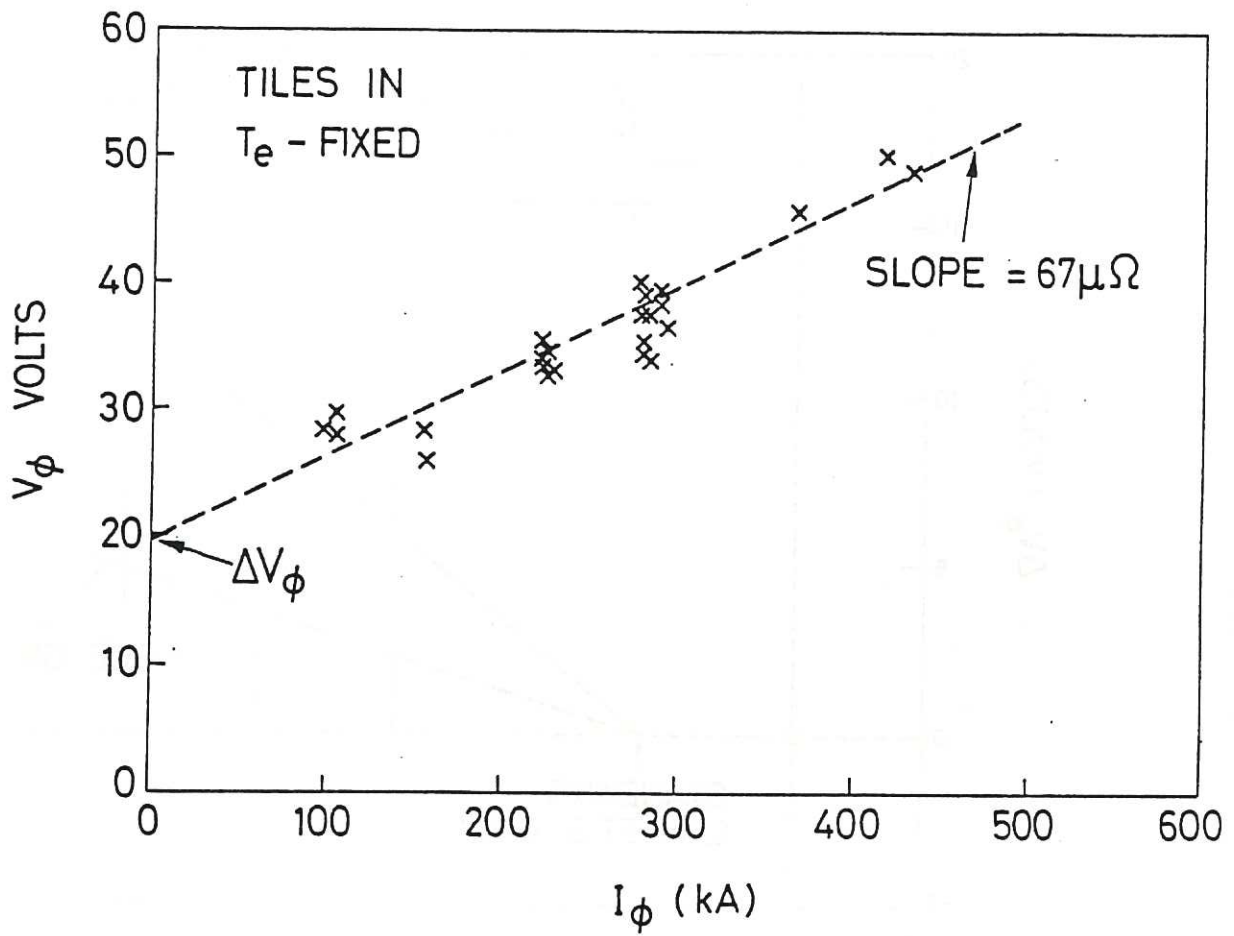


Figure 1 Dependence of measured loop voltage on plasma current before the limiter removal. All data are for T_e (on-axis) in the range $250 \pm 35\text{eV}$. The plasma resistance determined from the slope ($67 \mu\Omega$) is in good agreement with the estimated Spitzer value.

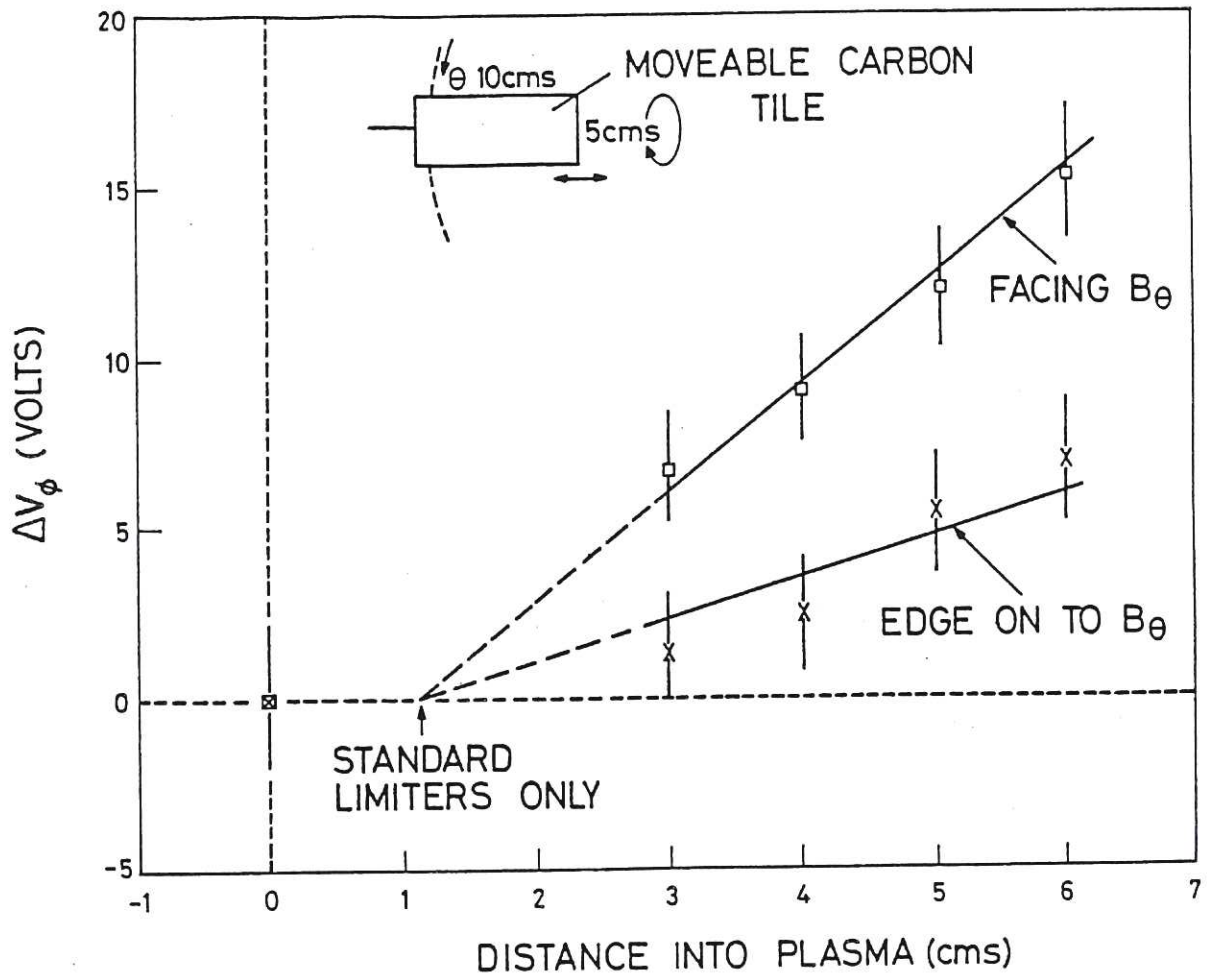


Figure 2 The increase in loop voltage, ΔV_ϕ , from the normal value of 33V, as a function of the insertion distance into the plasma of a moveable carbon tile limiter. The set up is shown schematically in the inset.

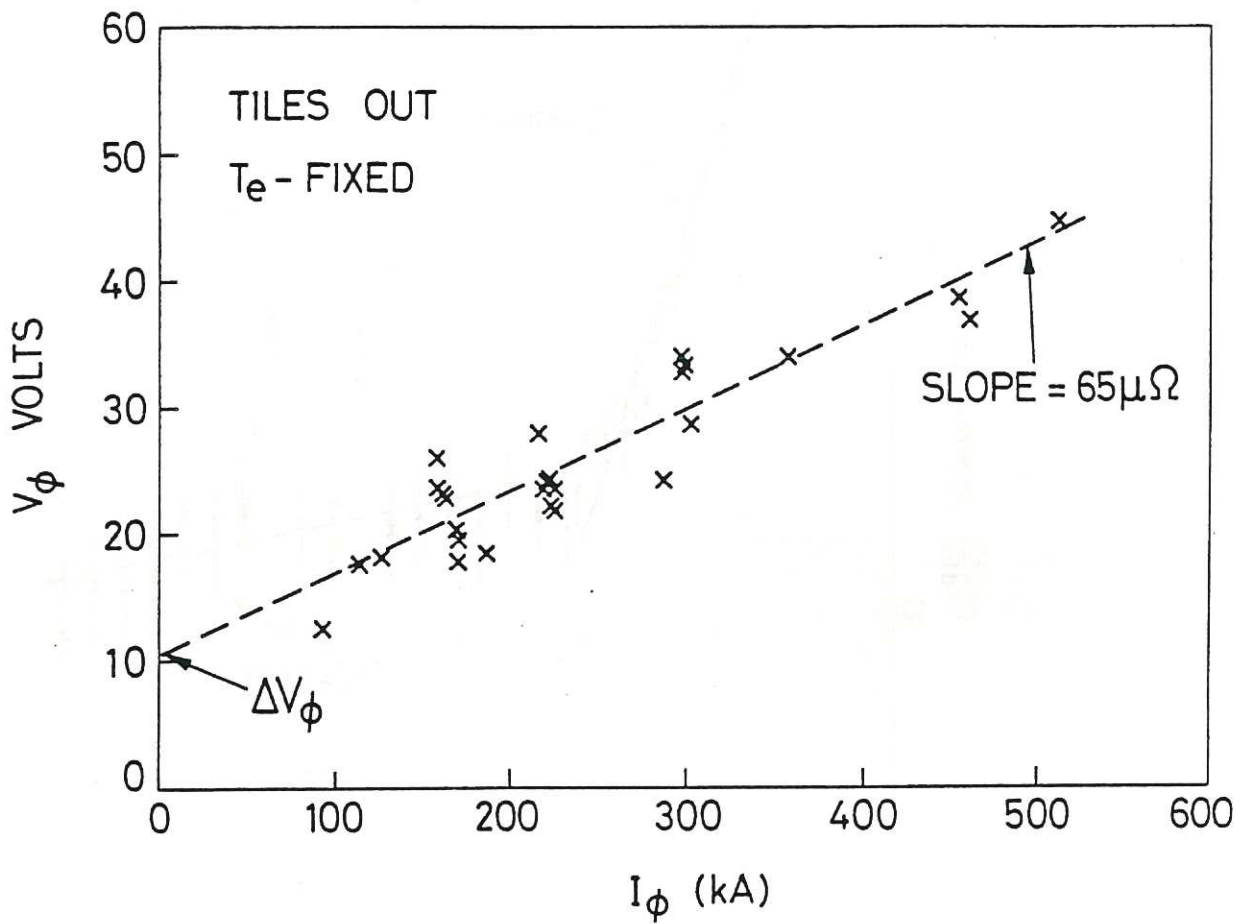


Figure 3 As Fig. 1 but after removal of the tile limiters and for T_e on-axis in the range $340 \pm 35\text{eV}$. The plasma resistance from the slope ($65 \mu\Omega$) is again in good agreement with the estimated Spitzer value. The reduction of 10V in the intercept compared with Fig. 1 is consistent with model predictions.

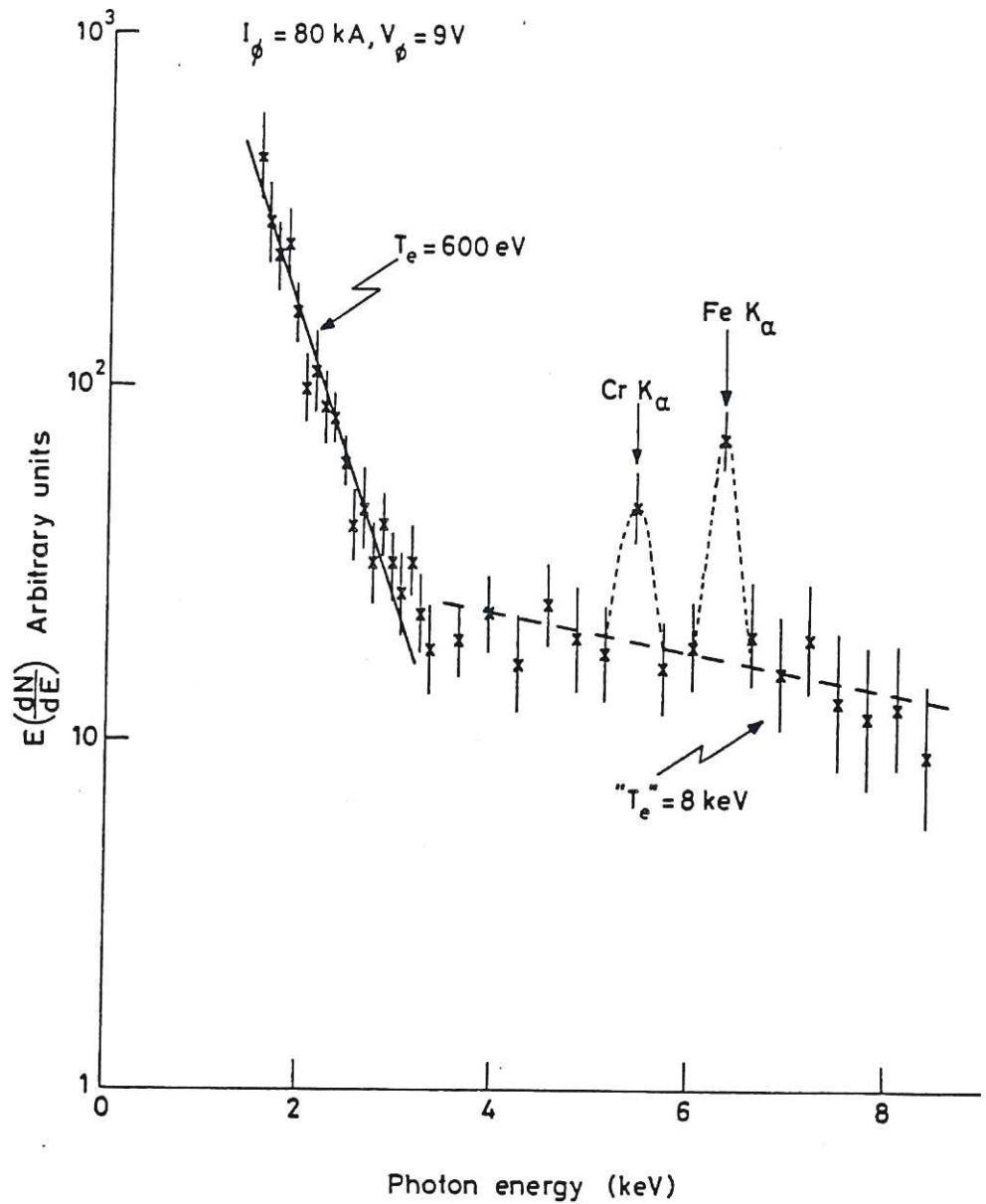


Figure 4 Soft X-ray pulse height spectrum from low density data ($< 3 \cdot 10^{18} \text{ m}^{-3}$) at $I_\phi = 80 \text{ kA}$. The suprathermal tail observed above 3 keV in photon energy corresponds to $\sim 1\%$ of the electron population. Chromium and iron impurity lines from the stainless steel liner are also observed.

